

Panchromatic squaraine compounds for broad band light harvesting electronic devices†

Luca Beverina,^{*a} Riccardo Ruffo,^a Matteo M. Salamone,^a Elisabetta Ronchi,^a Maddalena Binda,^b Dario Natali^{bc} and Marco Sampietro^{bc}

Received 29th November 2011, Accepted 19th January 2012

DOI: 10.1039/c2jm16240g

Squaraine compounds are currently investigated as high performance active components in both organic and hybrid photovoltaic devices as well as in photodetectors. Their most valuable features include a particularly efficient optical absorption in the Vis-NIR region, high polarizability, and a remarkable chemical stability. Their full exploitation is somewhat limited by a negligible absorption in the UV-Vis region (prototypical squaraines basically do not absorb below 500 nm). The aim of the present paper is the design and synthesis of truly panchromatic squaraines to be effectively employed as the photoactive materials in Vis operating optoelectronic devices. Our strategy involves the design of squaraines that are both nonsymmetric and core-substituted with suitable electron-withdrawing groups. We show the effect of such a design strategy by means of UV-Vis spectroscopy, cyclic voltammetry and prototypical device performances rationalization.

Introduction

1,3-Squaraines (or squarylium dyes) are the condensation product of squaric acid and two equivalents of a suitable electron rich precursor (anhydrobase or an activated arene).^{1–3} The use of two different electron rich precursors leads—through a variety of different multi-step procedures⁴—to nonsymmetric squaraines. Both symmetric and nonsymmetric squaraines are highly delocalized conjugated materials possessing a cyanine-like structure.^{5–7} Their most notable features are a strong and localized absorption in the Vis-NIR region, solubility in low polarity solvents, remarkable chemical stability, photoconducting capabilities and in some cases a strong NIR fluorescence.^{8,9} Squaraines have thus been employed in a number of technologically relevant research fields including: non-linear optics,^{10–12} highly stable NIR-fluorescent dyes,^{13,14} photopatterning,¹⁵ bioimaging,¹⁶ fluorescent ratiometric bioprobes,¹⁷ photodynamic therapy,^{18–21} field effect transistors,²² chemiluminescent materials,²³ bulk-heterojunction^{24–28} and hybrid^{29–31} solar cells and organic photodetectors.^{32,33}

Concerning their application in optoelectronic devices, the main appeal of squaraines as active media is their extremely efficient absorption. In addition, as a consequence of the

pronounced electron-withdrawing nature of the squarylium core, squaraines usually possess a low-lying HOMO level.^{24,27} In the Bulk Heterojunction configuration this is an additional value as the maximum voltage that a solar cell can generate (the Open Circuit Voltage) is proportional to the difference in energy between the HOMO of the donor material (the squaraine) and the LUMO of the accepting one (in the most common embodiment the acceptor is a fullerene derivative).³⁴

So far, squaraines demonstrated moderate to high efficiencies in both Bulk Heterojunction Solar Cells (with top performances averaging at 4.5%)²⁵ and dye sensitized solar cells (most efficient derivatives approach 6.5%).³⁰ Moreover, squaraines behave as very efficient active media, again in a Bulk Heterojunction configuration along with [6,6]-Phenyl C₆₁ butyric acid methyl ester (PC₆₁BM) as the acceptor, in high performance and remarkably stable organic NIR photodetectors, a class of devices working according to the same principle of solar cells.^{32,33,35,36} In this particular field, squaraines are unsurpassed in terms of absolute performances and environmental stability, even under strong operating bias.³³

One relevant issue affecting squaraines is that their extremely narrow absorption band leads to photon harvesting essentially localized in the Vis-NIR region. Even in the solid state, when a pronounced tendency to aggregation causes a relevant band broadening, the absorption below 500 nm is negligible.³⁷ Within this context, the use of nonsymmetric squaraines, instead of the definitely more common (and synthetically accessible) symmetric ones, is helpful as it introduces a certain charge-transfer contribution in the otherwise completely delocalized HOMO–LUMO optical transition. This translates into a remarkable broadening of the absorption band.¹⁰

^aDepartment of Materials Science and INSTM, University of Milano-Bicocca, Via Roberto Cozzi 53, 20125 Milano, Italy. E-mail: luca.beverina@mater.unimib.it

^bCenter for Nano Science and Technology @Polimi, Istituto Italiano di tecnologia, Via Pascoli 70/3, 20133 Milano, Italy

^cPolitecnico di Milano, Dipartimento di Elettrotecnica e Informazione, Piazza Leonardo Da Vinci 32, 20133 Milano, Italy

† Electronic supplementary information (ESI) available: Copy of the ¹H and ¹³C NMR for all new materials. See DOI: 10.1039/c2jm16240g

Another valuable strategy to increase the squaraine photon harvesting capabilities, particularly regarding the high-energy portion of the solar spectrum, requires the introduction of an electron withdrawing substituent directly on the squarylium core. This functionalization strategy, originally introduced by Tatarets and Terpetschnig,³⁸ provides the squaraine with an additional high-energy absorption, beneficial in both the DSSC³⁹ and BHJ⁴⁰ solar cell configurations. Recently, it has also been shown that this strategy provides bright NIR emitting dyes.⁴¹

For example, we have shown that the absorption spectrum of the anhydrobase derived symmetric squaraine **1** (Scheme 1) shows the typical strong and sharp absorption band arising from the cyanine-like transition associated with the delocalization of the nitrogen lone pair all over the main conjugation axis of the molecule. The core substituted derivative **2** (Scheme 1) displays the same low energy band and a new high energy one attributed to the core functionalization.³⁹

The aim of the present paper is the preparation of two squaraines of general formula **3** that are at the same time nonsymmetric (and thus possessing a broadened low energy absorption) and core substituted (in order to observe the additional high energy absorption band) to be employed as panchromatic sensitizers in organic light harvesting devices operating in the BHJ configuration (Scheme 1).

Experimental

1. Synthesis of the materials

Symmetric squaraines can be prepared by the direct reaction, under a variety of conditions, of two equivalents of the electron-rich precursor and squaric acid.³⁷ Conversely, the preparation of a nonsymmetric squaraine is a multi-step process that involves the isolation of the condensation product of one equivalent of the first electron rich material with a suitable squaric acid derivative.⁴

Particularly activated arenes such as 2,4-dimethylpyrrole (**4**) are able to react with squaric acid esters to give the corresponding emisquarate in good yield. Thus, derivative **4** was reacted with stoichiometric ethylsquarate in refluxing ethanol to

give the emisquarate **6** as a yellow solid. This can be easily converted to the corresponding emisquaraine **9** by hydrolysis in a 1 M LiOH THF solution, followed by acidification.¹⁰ The emisquaraine **9** was then converted into the nonsymmetric squaraine **sq-CO** in good yield, by reaction with the anhydrobase generated *in situ* by the action of imidazole on the salt **11**, according to the previously published procedure (Scheme 2).¹⁰

The emisquarate **6** is also the common intermediate for the preparation of the core-substituted derivatives **sq-CN** and **sq-PY**. In detail, **6** was condensed with malononitrile in refluxing ethanol in the presence of excess triethylamine. The substituted emisquaraine **8** was precipitated by acidification of the reaction mixture with excess 5% HCl to give the pure compound as a yellow-orange precipitate. Derivative **8** is a strong acid and is highly soluble in water; an excess of HCl is needed in order to trigger its precipitation. Finally, **8** was reacted with **11** in the presence of stoichiometric imidazole in a 3 : 1 refluxing mixture of ⁱPrOH and toluene under a Dean–Stark trap. The nonsymmetric squaraine **sq-CN** was isolated in 25% yield as a deep blue, shiny solid (Scheme 2).

The reaction of **6** with 3-methyl-1-phenyl-pyrazol-5-one **7** in refluxing ethanol in the presence of excess triethylamine gave, after acidification, the substituted emisquaraine **10** in good yield as a yellow-brown solid. In the last step, **10** was reacted with **12** in the presence of stoichiometric imidazole in a ⁱPrOH:toluene 1 : 1 refluxing mixture to give the squaraine **sq-PY** after chromatographic purification (Scheme 2).

Interestingly, the reaction of **7** with the dimethylindolenine derived emisquarate **15**, under the same conditions employed for the preparation of **10**, only gave the corresponding, core unsubstituted, emisquaraine **16** (Scheme 3).

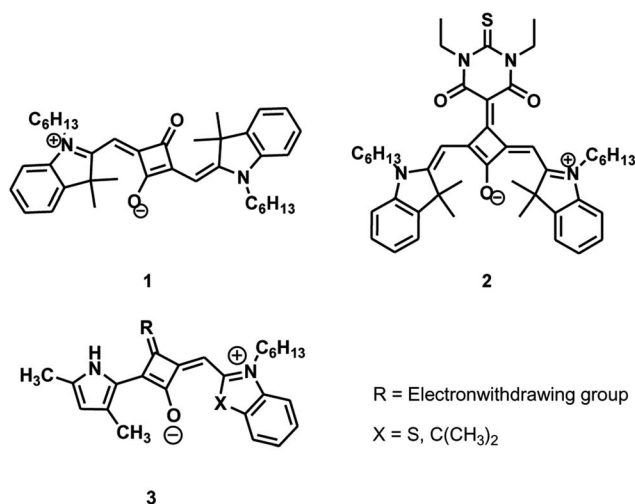
2. UV-Vis characterization

Squaraine **sq-CO** was originally synthesized as a Second Harmonic Generating molecule in the context of nonlinear optics. Our previous investigation shows that **sq-CO** is a moderately polar molecule possessing a Full Width at Half Maximum (FWHM) of 894 cm⁻¹ in CHCl₃ and moderate solvatochromic effect.¹⁰

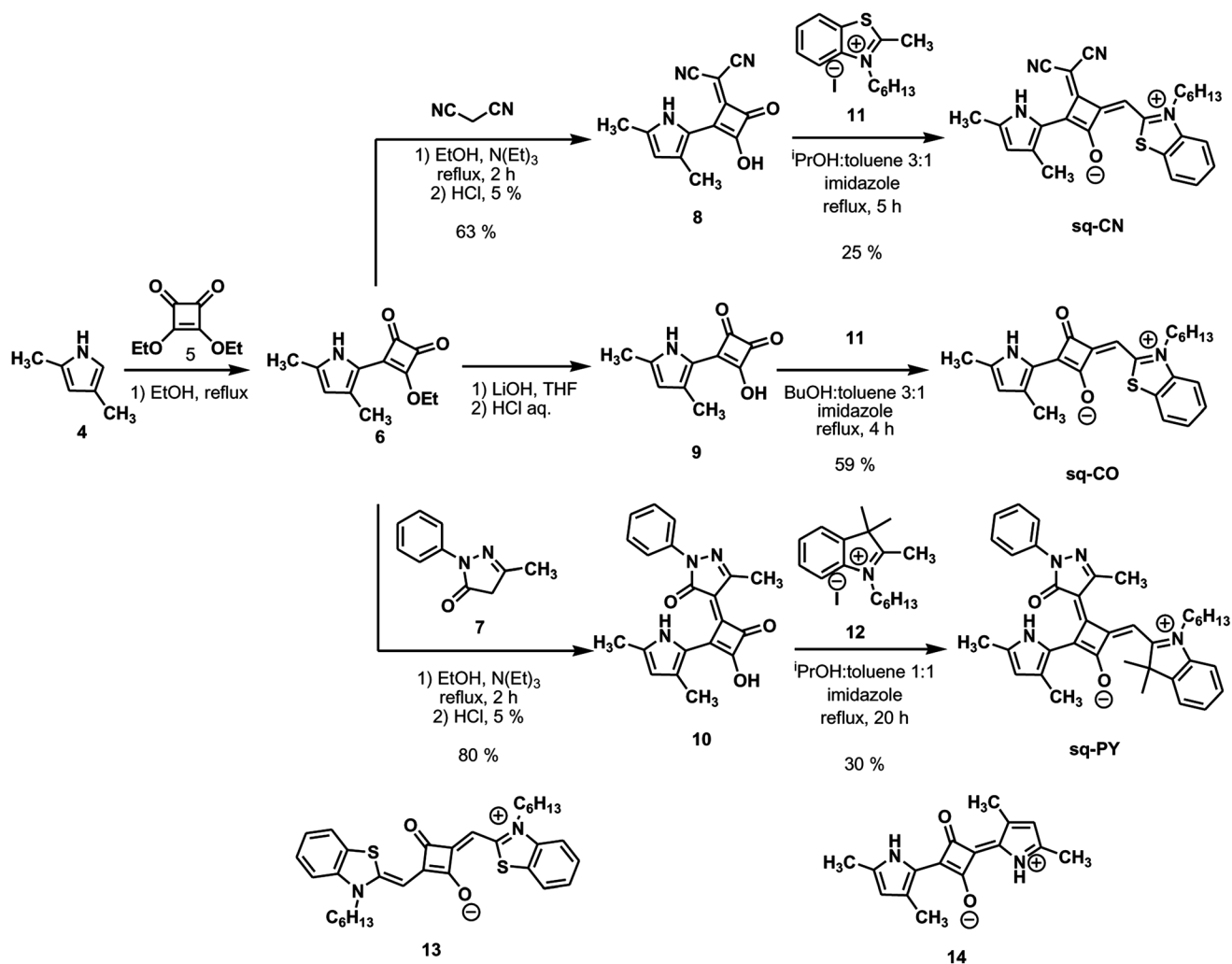
Fig. 1 shows the comparison between the absorption spectra of **sq-CO** and the corresponding symmetric squaraines **13** (derived from the benzothiazolium anhydrobase)²¹ and **14** (derived from 2,4-dimethylpyrrole).¹ The HOMO–LUMO gap of **sq-CO** is intermediate between that of **14** and **13** but its FWHM is larger than both of them (see Table 1).

These favourable features, along with a relatively simple and high yield synthetic access, made **sq-CO** the ideal structure to study the influence of core functionalization on optical and optoelectronic properties. Fig. 2 shows the comparison between the absorption spectra of squaraine **sq-CO** and the core-substituted squaraine **sq-CN**. Both the position and the FWHM of the main cyanine-like absorption band are only marginally affected by the presence of the substituent.

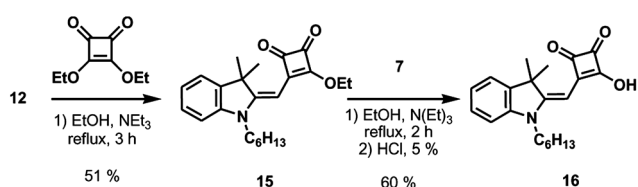
Indeed, **sq-CN** possesses a second absorption band in the 350–400 nm region. Such a band is connected with the presence of the malononitrile group and can be described as the merocyanine-like oscillator due to the delocalization of the core negative charge between the oxygen atom and the malononitrile moiety.



Scheme 1



Scheme 2



Scheme 3

This interpretation is coherent with our previous computational investigation of a dimethylindolenine-based core substituted squaraine.³⁹

In order to both increase the relative intensity of the high-energy peak and possibly further broaden the main absorption band, we replaced the malononitrile residue with a more conjugated and nonsymmetric acceptor, the 3-methyl-1-phenyl-pyrazol-5-one 7, thus giving the derivative sq-PY.

Fig. 3 shows the comparison between the absorption spectra of squaraines sq-CN and sq-PY. The pyrazolone-substituted derivative shows three distinct absorption bands. The main cyanine-like transition falls at the exact same energy as that of sq-CN, its FWHM however goes from the 1450 cm⁻¹ of the former

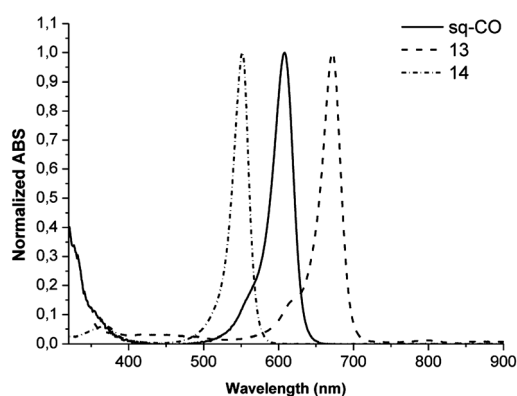
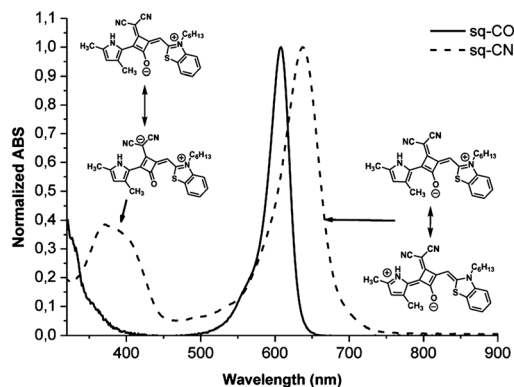
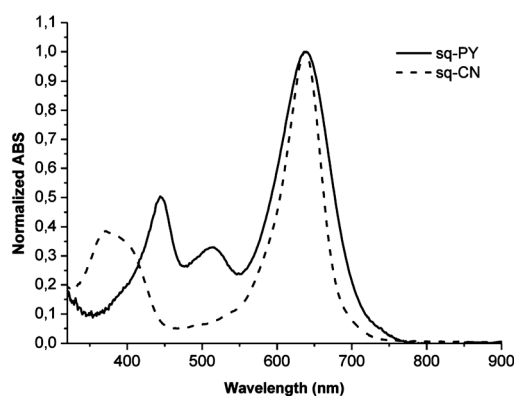


Fig. 1 Comparison between the absorption spectra (CH₂Cl₂) of the symmetric squaraines 13 and 14 and the nonsymmetric derivative sq-CO.

to a very remarkable (for a squaraine compound) 2121 cm⁻¹. At the same time a new band is formed at 510 nm. sq-PY is thus able to absorb all over the visible spectrum. To the best of our knowledge, this is an unprecedented result for squaraine compounds.

Table 1 UV-Vis characterization data for squaraines **sq-CO**, **sq-CN** and **sq-PY**

| | λ_{\max} (1)/nm | λ_{\max} (2)/nm | ϵ/l cm ⁻¹ mol ⁻¹ | FWHM/cm ⁻¹ |
|--------------|-------------------------|-------------------------|---|-----------------------|
| 14 | 672 | — | 295 000 | 668 |
| 15 | 552 | — | 79 000 | 797 |
| sq-CO | 608 | — | 230 000 | 894 |
| sq-CN | 638 | 368 | 118 000 | 1450 |
| sq-PY | 637 | 444, 514 | 81 000 | 2121 |

**Fig. 2** Comparison between the absorption spectra (CHCl₃) of the nonsymmetric squaraine **sq-CO** and that of the core substituted squaraine **sq-CN**.**Fig. 3** Comparison between the UV-Vis absorption spectra of CHCl₃ solutions of the cross-substituted nonsymmetric squaraines **sq-CN** and **sq-PY**.

Derivative **sq-PY** could in principle be obtained as a mixture of isomers having the pyrazolone ring oriented in both the possible ways.

The NMR characterization clearly shows that the chromatographic purification enables to isolate one single isomer (see ESI[†]). NMR also shows that the precursor of **sq-PY**, the emisquaraine **10**, is formed too as a single isomer. In this case no purification step is involved and the particularly high reaction yield ensures that the reaction is almost completely stereoselective.

The unambiguous assignment of the structure of **sq-PY** would require a single crystal X-ray characterization. Unfortunately, we did not succeed in growing high quality crystals for this

purpose. The tentative, unverified assignment of the specific regioisomer we show is based on the chemical shift of the pyrrolic N–H signal that falls at 6.05 ppm, very far from its usual position between 10 and 9 ppm. We attributed this uncommon high-field shift to the establishment of a hydrogen bond between the pyrrolic N–H and the pyrazolone carbonyl residue.

The establishment of such a hydrogen-bond could be the reason for both the high yield and the stereoselectivity of the condensation reaction between the emisquarate **6** and the pyrazolone **7**.

3. Electrochemical characterization

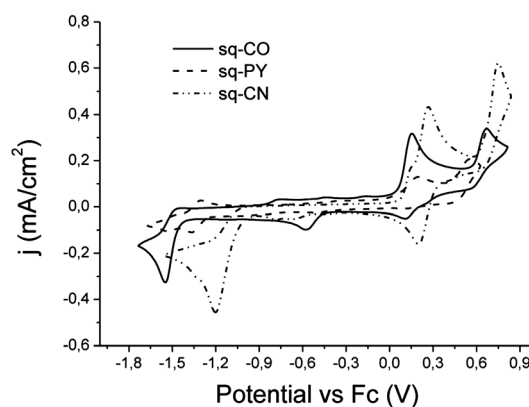
Cyclic voltammetry (CV) gives an immediate insight into the electronic effects induced by the presence of the electron-withdrawing group on the squarylium core.

Fig. 4 shows the comparison between the CV plots for the three squaraines considered in the present work. The three voltammograms show similar features. At positive potentials the plots show two waves corresponding to the oxidation of the two electron rich moieties: the anhydrobase and the dimethylpyrrole. In the case of both **sq-CO** and **sq-PY** such processes are irreversible. Conversely, in the case of **sq-CN** the process is quasi reversible.

Indeed, we recorded Differential Pulsed Voltammetry (DPV) plots for all of the compounds, as this is the most appropriate technique to characterize partially or completely irreversible processes (Fig. 5).

The peaks of the first oxidation process in the DPV plots are shifted progressively towards more positive potentials in the series **sq-CO**, **sq-PY**, **sq-CN**. This is in agreement with the electron withdrawing capabilities of the substituent, contributing to the enhancement of the accepting nature of the squarylium core. The peaks of the first reduction process are shifted towards less negative potentials in the series **sq-CN**, **sq-PY**, **sq-CO**. In the case of **sq-PY** the reduction process becomes fully reversible.

From the standpoint of their use in photodetecting/photovoltaic devices, both **sq-CN** and **sq-PY** show promising features, regarding their low lying HOMO levels. However, we focused our attention on derivative **sq-PY** as it ensures both a very efficient photon harvesting all over the visible spectrum and a LUMO level

**Fig. 4** Cyclic voltammetry plots for squaraines **sq-CO**, **sq-CN**, **sq-PY** in CH₃CN with tetrabutylammonium hexafluorophosphate as the supporting electrolyte.

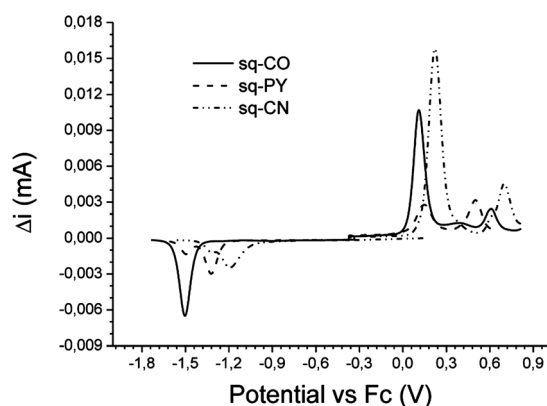


Fig. 5 DPV plots for squaraines **sq-CO**, **sq-CN** and **sq-PY** in CH_3CN with tetrabutylammonium hexafluorophosphate as the supporting electrolyte.

that is slightly above that of PC_{61}BM . Conversely, the **sq-CN** LUMO is slightly below than that of PC_{61}BM , thus in principle unsuitable for the photoinduced electron transfer process.

Table 2 summarizes the most relevant electrochemical properties of **sq-CO**, **sq-CN** and **sq-PY** highlighting both the low lying position of their HOMO levels with respect to P_3HT and the progressive shift of the LUMO energies towards that of PC_{61}BM .

4. Device assembly and testing

In order to test the capability of **sq-PY** to act as the photosensitizer in light harvesting applications, we prepared a device based on the classical sandwich-like structure depicted in Fig. 6, where the squaraine is used as the donor material in bulk-heterojunction configuration with PC_{61}BM as the acceptor.

A **sq-PY**: PC_{61}BM 1 : 3 by weight ratio was chosen since this particular composition gave the best performance for squaraine- PC_{61}BM bulk-heterojunction based active materials.^{27,32,33}

Fig. 7 shows the device electrical characterization. In particular, Fig. 7a shows the dark currents of the device as a function of the externally applied bias voltage. Clear rectification can be observed, with a 10^3 ratio between current in forward bias (negative voltages in the plot) and current in reverse bias (positive voltages in the plot), both evaluated at 1 V. Fig. 7b shows the photon-to-electron conversion efficiency (External Quantum Efficiency—EQE) of the device, reverse biased at 1 V, displayed as a function of the illumination wavelength. The EQE curve is always higher than 3% all over the visible spectrum (400–750 nm). This result clearly demonstrates that **sq-PY** can be used as a truly panchromatic sensitizer, as all of its three absorption bands are capable of generating a photocurrent.

Table 2 **sq-CO**, **sq-CN** and **sq-PY** in CH_3CN with tetrabutylammonium *p*-toluenesulfonate as the supporting electrolyte. Electrochemical HOMO and LUMO levels

| Compound | $E_{1/2}$ (1)/V | $E_{\text{pc}}^{\text{red}}/\text{V}$ | HOMO | LUMO |
|--------------------------------|-----------------|---------------------------------------|-------|-------|
| sq-CO | 0.11 | -1.50 | -5.31 | -3.70 |
| sq-CN | 0.22 | -1.19 | -5.42 | -4.01 |
| sq-PY | 0.15 | -1.32 | -5.35 | -3.88 |
| P_3HT | — | — | -5.00 | -3.30 |
| $\text{PC}_{61}\text{BM}^{42}$ | — | — | -5.93 | -3.91 |

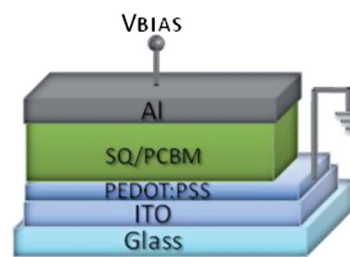


Fig. 6 Sketch of the device based on the **sq-PY**: PC_{61}BM bulk-heterojunction active material.

The device is still working in the NIR-IR region with efficiencies as high as 0.5% at 850 nm.

Materials. All chemicals and solvents were purchased from Fluka or Aldrich and used as received unless explicitly stated. ^1H spectra were recorded using a Bruker AMX-500 spectrometer. ^{13}C NMR spectra were recorded on a Bruker AMX-500 spectrometer operating at 125.70 MHz. Absorption spectroscopy was performed using a Jasco V570 spectrophotometer. Melting points are uncorrected.

Derivatives **6**,⁴ **7**,⁴³ **9**,⁴ **11**,⁴⁴ **12**,⁴⁵ **13**,²¹ **14** (ref. 1) and **15–16** (ref. 46) were prepared according to the published procedures.

2-(2-(3,5-Dimethyl-1H-pyrrol-2-yl)-3-hydroxy-4-oxocyclobut-2-enylidene)malononitrile **8**. A solution of the ethyl emisquarate **6** (1.55 g, 7.07 mmol), malononitrile (0.48 g, 7.27 mmol) and triethylamine (2.8 ml, 15 mmol) in absolute ethanol (30 ml) was refluxed for 4 h. The colour gradually turns from pale yellow to

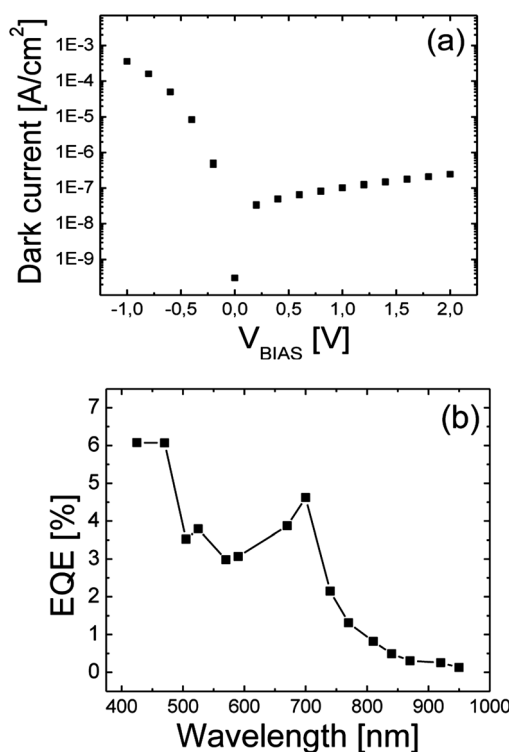


Fig. 7 (a) I - V characteristics under dark conditions and (b) External Quantum Efficiency as a function of wavelength for the device based on a 1 : 3 mixture of squaraine **sq-PY** and PC_{61}BM .

dark yellow-brown. The homogeneous dark solution was poured into 100 ml of 5% HCl, to give a deep yellow clear solution. After standing overnight at room temperature, a thick red precipitate was formed. Suction filtration gave the title compound as red needles (1.06 g, 4.43 mmol, 63% yield). Mp 140–142 °C (dec); ¹H NMR (DMSO-*d*₆) δ: 9.98 (1H, s), 7.19 (s, broad), 5.78 (1H, s), 2.27 (3H, s), 2.16 (3H, s). ¹³C δ: 193.4, 186.0, 176.6, 162.5, 134.3, 125.9, 120.5, 119.3, 118.6, 111.7, 13.5 (2C). Analysis calcd for C₁₃H₉N₃O₂: C, 65.27; H, 3.79; N, 17.56; calcd for C₁₃H₉N₃O₂·1H₂O: C, 60.70; H, 4.31; N, 16.33; found: C, 60.92; H, 4.40; N, 16.50%.

(*E*)-4-(2-(3,5-Dimethyl-1H-pyrrol-2-yl)-3-hydroxy-4-oxocyclobut-2-enylidene)-3-methyl-1-phenyl-1H-pyrazol-5(4H)-one **10**. A solution of the ethyl emisquarate **6** (1.53 g, 7.00 mmol), the pyrazolone **7** (1.26 g, 7.23 mmol) and triethylamine (2.7 ml, 14 mmol) in absolute ethanol (20 ml) was refluxed for 3 h. The colour gradually turns from pale yellow to dark yellow-brown. The homogeneous dark solution was poured into 300 ml of 5% HCl, to give a fine yellow precipitate. Suction filtration gave the title compound as a yellow powder that was dried in the vacuum at 50 °C till constant weight (1.94 g, 5.58 mmol, 80% yield). Mp 180–182 °C (dec); ¹H NMR (DMSO-*d*₆) δ: 7.76 (2H, d, *J* = 7.50), 7.55 (2H, t, *J* = 8.00), 7.37 (1H, t, *J* = 7.50), 5.98 (1H, s), 2.56 (3H, s), 2.48 (3H, s), 2.26 (3H, s). ¹³C δ: 193.8, 193.1, 173.7, 168.9, 160.1, 148.7, 141.3, 135.9, 133.8, 129.8, 127.3, 122.2, 119.7, 114.9, 97.2, 14.4, 14.2, 13.9. Analysis calcd for C₂₀H₁₇N₃O₃: C, 69.15; H, 4.93; N, 12.10; calcd for C₂₀H₁₇N₃O₃·½H₂O: C, 67.40; H, 5.09; N, 11.79; found: C, 67.00; H, 4.96; N, 11.77%.

Squaraine sq-CN. A suspension of the emisquaraine **8** (0.544 g, 1.90 mmol), the benzothiazolium salt **11** (0.710 g, 1.97 mmol) and imidazole (0.272 g, 4.00 mmol) in a 1 : 1 *n*-BuOH:toluene mixture (20 ml) was refluxed under a Dean–Stark trap. The colour gradually turns from yellow to deep green. After 6 h at the reflux temperature, the deeply coloured mixture was cooled at room temperature and a shiny purple precipitate was formed. Suction filtration gave a purple powder that was taken up with 5 ml of ethanol, stirred at rt for 24 h and filtered again to give the title compound as a dark precipitate (0.220 g, 0.48 mmol, 25% yield). Mp 215–217 °C. ¹H NMR (DMSO-*d*₆) δ: 10.36 (1H, s), 8.26 (1H, d, *J* = 8.00), 8.06 (1H, d, *J* = 8.50), 7.71 (1H, t, *J* = 8.50), 7.59 (1H, t, *J* = 8.00), 6.76 (1H, s), 5.93 (1H, s), 4.49 (2H, t, *J* = 8.00), 2.37 (3H, s), 2.22 (3H, s), 1.81 (2H, q, *J* = 8.00), 1.44 (2H, q, *J* = 8.00), 1.32–1.28 (4H, m), 0.87 (3H, t, *J* = 7.00). ¹³C δ: 206.9, 173.1, 167.8, 165.9, 161.8, 150.7, 140.9, 138.5, 130.7, 129.5, 129.1, 127.3, 124.3, 120.1, 119.6, 119.2, 115.7, 113.5, 92.2, 48.5, 31.2, 31.1, 28.3, 26.1, 22.4, 14.2, 13.7, 13.6. Anal calcd for C₂₇H₂₆N₄OS: C, 71.34; H, 5.76; N, 12.32; S, 7.05; found: C, 71.84; H, 5.75; N, 12.65; S, 7.20%.

Squaraine sq-PY. A suspension of the emisquaraine **10** (0.08 g, 0.23 mmol), derivative **12** (0.09 g, 0.24 mmol) and imidazole (0.017 g, 0.25 mmol) was refluxed in a 1 : 1 ¹PrOH:toluene mixture (20 ml) under a Dean–Stark trap. The colour slowly turns from deep yellow to dark green. After 20 h at the reflux temperature the solvent was removed under reduced pressure and the residue was purified by chromatography (SiO₂, AcOEt:CH₂Cl₂ 1 : 5) to give the pure title compound as a purple

wax. The product was dissolved in 20 ml of *n*-hexane and cooled at –78 °C. The purple precipitate thus formed was filtered in a cold Hirsh funnel and dried under vacuum (0.04 g, 0.07 mmol, 30% yield). Mp 90 °C; ¹H-NMR (acetone-*d*₆) δ: 8.30 (2H, d, *J* = 8.54), 7.61 (1H, d, *J* = 7.43), 7.48 (1H, d, *J* = 8.28), 7.46 (1H, t, *J* = 8.01), 7.39 (2H, t, *J* = 8.01), 7.34 (1H, t, *J* = 7.20), 7.11 (1H, t, *J* = 8.33), 6.19 (1H, s), 6.1–6.0 (1H, s-broad), 4.38 (2H, t, *J* = 8.00), 2.68 (3H, s), 2.41 (3H, s), 2.26 (3H, s), 1.87 (2H, q, *J* = 7.50), 1.70 (6H, s), 1.46 (2H, q, *J* = 7.50), 1.36–1.25 (4H, m), 0.84 (3H, t, *J* = 7.00). ¹³C-NMR (acetone-*d*₆) δ: 176.3, 175.0, 173.2, 164.0, 163.0, 161.7, 148.7, 146.3, 142.2, 142.0, 140.9, 128.3, 128.2, 125.5, 123.1, 122.6, 122.4, 118.8, 118.0, 111.7, 108.3, 95.2, 91.5, 50.3, 45.0, 31.2, 27.3, 26.2, 25.6, 22.3, 17.0, 13.8, 13.4. Anal calcd for: C₃₇H₄₀N₄O₂: C, 77.59; H, 7.04; N, 9.78; calcd for C₃₇H₄₀N₄O₂·½H₂O: C, 76.39; H, 7.10; N, 9.63; found: C, 76.61; H, 7.27; N, 9.27%.

Details on electrochemical characterization. Squaraines were dissolved (concentration about 10^{–4} M) in the supporting electrolyte that was a 0.1 M solution of tetrabutylammonium hexafluorophosphate (Fluka, electrochemical grade, ≥99.0%) in anhydrous acetonitrile (Aldrich, 99.8%). Differential Pulsed Voltammetry (DPV) and Cyclic Voltammetry (CV) were carried out at scan rate of 20 and 50 mV s^{–1}, respectively, using a PARSTA2273 potentiostat in a single chamber three electrodes electrochemical cell in a glove box filled with argon ([O₂] ≤ 1 ppm). The working, counter, and the pseudo-reference electrodes were a Au pin, a Pt flag and a Ag/AgCl wire, respectively. The Ag/AgCl pseudo-reference electrode was externally calibrated by adding ferrocene (1 mM) to the electrolyte.

Details on device preparation and characterization

Device structure: ITO-PEDOT:PSS-SQ:PCBM-Al. PEDOT:PSS (Clevios P VP AI 4083) was spin-coated from aqueous solution at 2000 rpm onto clean glass-ITO substrates pre-treated with oxygen plasma. Following the deposition, a thermal treatment at 100 °C for 15 minutes under nitrogen was applied. The sq-PY:PC₆₁BM 1 : 3 by weight blend was dissolved in chloroform (19.2 mg ml^{–1}) and spin-coated at 100 rpm in a glovebox for 1 minute (followed by 1 minute at 1000 rpm). Al was evaporated at 10^{–6} mbar. Device active area: 4 mm².

All electrical measurements were performed in vacuum (below 10^{–6} mbar).

Dark currents were recorded through a Keithley SCS4200. For the quantum efficiency measurements, the device was reverse biased at 1 V and irradiated by means of a set of light emitting diodes (LEDs) providing 500 μs long light pulses. The resulting photocurrent was read by connecting the device to a low-noise transimpedance amplifier. The EQE was calculated as the ratio of the number of collected charges, determined by integrating the transient output photocurrent during the radiation pulse, and the number of incident photons, obtained by calibrating the LEDs (giving a light intensity of about 30 mW cm^{–2}) by means of a silicon photodetector.

Conclusions

We successfully designed and synthesized core substituted squaraine compounds possessing a panchromatic absorption.

The electrochemical characterization shows that core substitution is an efficient strategy for the tuning of the HOMO and LUMO levels position in squaraine compounds. Dealing with optical properties, core substitution leads to the formation of a high-energy band within a region where standard squaraine sensitizers do not absorb. In the case of **sq-PY** both absorption and photocurrent generation are efficient all over the visible spectrum.

Acknowledgements

This paper is dedicated to the memory of Dr Miriam Ferrari. We acknowledge INSTM (PRISMA2007) and MURST (FIRB 2003: Molecular compounds and hybrid nanostructured materials with resonant and non-resonant optical properties for photonic devices) for financial support.

Notes and references

- 1 A. Treibs and K. Jacob, *Angew. Chem., Int. Ed. Engl.*, 1965, **4**, 694.
- 2 A. Treibs and K. Jacob, *Justus Liebigs Ann. Chem.*, 1968, **712**, 123–137.
- 3 A. Treibs and K. Jacob, *Justus Liebigs Ann. Chem.*, 1966, **699**, 153–167.
- 4 D. Keil and H. Hartmann, *Dyes Pigm.*, 2001, **49**, 161–179.
- 5 L. Beverina and P. Salice, *Eur. J. Org. Chem.*, 2010, 1207–1225.
- 6 A. Ajayaghosh, *Acc. Chem. Res.*, 2005, **38**, 449–459.
- 7 S. Sreejith, P. Carol, P. Chithra and A. Ajayaghosh, *J. Mater. Chem.*, 2008, **18**, 264.
- 8 K. Y. Law, *J. Phys. Chem.*, 1987, **91**, 5184–5193.
- 9 K. Y. Law and F. C. Bailey, *J. Org. Chem.*, 1992, **57**, 3278–3286.
- 10 L. Beverina, R. Ruffo, G. Patriarca, F. De Angelis, D. Roberto, S. Righetto, R. Ugo and G. A. Pagani, *J. Mater. Chem.*, 2009, **19**, 8190–8197.
- 11 L. Beverina, M. Crippa, P. Salice, R. Ruffo, C. Ferrante, I. Fortunati, R. Signorini, C. M. Mari, R. Bozio, A. Facchetti and G. A. Pagani, *Chem. Mater.*, 2008, **20**, 3242–3244.
- 12 C.-T. Chen, S. R. Marder and L.-T. Cheng, *J. Am. Chem. Soc.*, 1994, **116**, 3117–3118.
- 13 J. R. Johnson, N. Fu, E. Arunkumar, W. M. Leevy, S. T. Gammon, D. Piwnica-Worms and B. D. Smith, *Angew. Chem., Int. Ed.*, 2007, **46**, 5528–5531.
- 14 E. Arunkumar, C. C. Forbes, B. C. Noll and B. D. Smith, *J. Am. Chem. Soc.*, 2005, **127**, 3288–3289.
- 15 L.-H. Liu, K. Nakatani, R. Pansu, J.-J. Vachon, P. Tauc and E. Ishow, *Adv. Mater.*, 2007, **19**, 433–436.
- 16 Z. Xiang, E. E. Nesterov, J. Skoch, T. Lin, B. T. Hyman, T. M. Swager, B. J. Bacskai and S. A. Reeves, *J. Histochem. Cytochem.*, 2005, **53**, 1511–1516.
- 17 S. Sreejith, K. P. Divya and A. Ajayaghosh, *Angew. Chem., Int. Ed.*, 2008, **47**, 7883–7887.
- 18 E. Arunkumar, P. K. Sudeep, P. V. Kamat, B. C. Noll and B. D. Smith, *New J. Chem.*, 2007, **31**, 677–683.
- 19 V. Rapozzi, L. Beverina, P. Salice, G. A. Pagani, M. Camerin and L. E. Xodo, *J. Med. Chem.*, 2010, **53**, 2188–2196.
- 20 D. Ramaiah, I. Eckert, K. T. Arun, L. Weidenfeller and B. Epe, *Photochem. Photobiol.*, 2004, **79**, 99–104.
- 21 P. F. Santos, L. V. Reis, P. Almeida, J. P. Serrano, A. S. Oliveira and L. F. Vieira Ferreira, *J. Photochem. Photobiol., A*, 2004, **163**, 267–269.
- 22 E. C. P. Smits, S. Setayesh, T. D. Anthopoulos, M. Buechel, W. Nijssen, R. Coehoorn, P. W. M. Blom, B. de Boer and D. M. de Leeuw, *Adv. Mater.*, 2007, **19**, 734–738.
- 23 J. M. Baumes, J. J. Gassensmith, J. Giblin, J.-J. Lee, A. G. White, W. J. Culligan, W. M. Leevy, M. Kuno and B. D. Smith, *Nat. Chem.*, 2010, **2**, 1025–1030.
- 24 L. Beverina, M. Drees, A. Facchetti, M. Salamone, R. Ruffo and G. A. Pagani, *Eur. J. Org. Chem.*, 2011, 5555–5563.
- 25 G. Wei, S. Wang, K. Sun, M. E. Thompson and S. R. Forrest, *Adv. Energy Mater.*, 2011, **1**, 184–187.
- 26 D. Bagnis, L. Beverina, H. Huang, F. Silvestri, Y. Yao, H. Yan, G. A. Pagani, T. J. Marks and A. Facchetti, *J. Am. Chem. Soc.*, 2010, **132**, 4074–4075.
- 27 F. Silvestri, M. D. Irwin, L. Beverina, A. Facchetti, G. A. Pagani and T. J. Marks, *J. Am. Chem. Soc.*, 2008, **130**, 17640–17641.
- 28 F. Silvestri, I. López-Duarte, W. Seitz, L. Beverina, M. V. Martínez-Díaz, T. J. Marks, D. M. Guldi, G. A. Pagani and T. Torres, *Chem. Commun.*, 2009, 4500–4502.
- 29 J.-H. Yum, P. Walter, S. Huber, D. Rentsch, T. Geiger, F. Nüesch, F. De Angelis, M. Grätzel and M. K. Nazeeruddin, *J. Am. Chem. Soc.*, 2007, **129**, 10320–10321.
- 30 S. Paek, H. Choi, C. Kim, N. Cho, S. So, K. Song, M. K. Nazeeruddin and J. Ko, *Chem. Commun.*, 2011, **47**, 2874–2876.
- 31 Y. Shi, R. B. M. Hill, J.-H. Yum, A. Dualeh, S. Barlow, M. Grätzel, S. R. Marder and M. K. Nazeeruddin, *Angew. Chem., Int. Ed.*, 2011, **50**, 6619–6621.
- 32 M. Binda, A. Iacchetti, D. Natali, L. Beverina, M. Sassi and M. Sampietro, *Appl. Phys. Lett.*, 2011, **98**, 073303.
- 33 M. Binda, T. Agostinelli, M. Caironi, D. Natali, M. Sampietro, L. Beverina, R. Ruffo and F. Silvestri, *Org. Electron.*, 2009, **10**, 1314–1319.
- 34 J. Peet, A. J. Heeger and G. C. Bazan, *Acc. Chem. Res.*, 2009, **42**, 1700–1708.
- 35 S. Sahu and A. Pal, *J. Appl. Phys.*, 2006, **99**, 114503-1–114503-4.
- 36 S. Sahu and A. Pal, *Mater. Sci. Eng., C*, 2007, **27**, 746–749.
- 37 K. Y. Law, *Chem. Rev.*, 1993, **93**, 449–486.
- 38 A. Tatarets, I. Fedyunyaeva, E. Terpetschnig and L. Patsenker, *Dyes Pigm.*, 2005, **64**, 125–134.
- 39 L. Beverina, R. Ruffo, C. M. Mari, G. A. Pagani, M. Sassi, F. De Angelis, S. Fantacci, J.-H. Yum, M. Grätzel and M. K. Nazeeruddin, *ChemSusChem*, 2009, **2**, 621–624.
- 40 U. Mayerhöffer, K. Deing, K. Gruss, H. Braunschweig, K. Meerholz and F. Würthner, *Angew. Chem., Int. Ed.*, 2009, **48**, 8776–8779.
- 41 U. Mayerhöffer, B. Fimmel and F. Würthner, *Angew. Chem., Int. Ed.*, 2011, **50**, 1–5.
- 42 Y. He, G. Zhao and B. Peng, *Adv. Funct. Mater.*, 2010, **20**, 3383–3389.
- 43 J. Deruiter, D. A. Carter, W. S. Arledge and P. J. Sullivan, *J. Heterocycl. Chem.*, 1987, **24**, 149–153.
- 44 E. Ronchi, R. Ruffo, S. Rizzato, A. Albinati, L. Beverina and G. A. Pagani, *Org. Lett.*, 2011, **13**, 3166–3169.
- 45 A. C. Pardal, S. S. Ramos, P. F. Santos, L. V. Reis and P. Almeida, *Molecules*, 2002, **7**, 320–330.
- 46 D. Scherer, R. Dörfler, A. Feldner, T. Vogtmann, M. Schwoerer, U. Lawrentz, W. Grahn and C. Lambert, *Chem. Phys.*, 2002, **279**, 179–207.